Journal of Applied Fluid Mechanics, Vol. 12, No. 2, pp. 391-402, 2019.
Available online at www.jafmonline.net, ISSN 1735-3572, EISSN 1735-3645.
DOI: 10.29252/jafm.12.02.28923

A Numerical Analysis of Laminar Forced Convection and Entropy Generation of a Diamond-Fe_3O_4/Water Hybrid Nanofluid in a Rectangular Minichannel

C. Uysal[1†], E. Gedik[2] and A. J. Chamkha[3,4]

[1] *Automotive Technologies Program, TOBB Vocational School of Technical Sciences, Karabuk University, Karabuk, 78050, Turkey*
[2] *Energy Systems Engineering, Technology Faculty, Karabuk University, Karabuk, 78050, Turkey*
[3] *Mechanical Engineering Department, Prince Sultan Endowment for Energy and Environment, Prince Mohammad Bin Fahd University, Al-Khobar 31952, Saudi Arabia*
[4] *RAK Research and Innovation Center, American University of Ras Al Khaimah, United Arab Emirates*

†*Corresponding Author Email: cuneytuysal@karabuk.edu.tr*

(Received February 24, 2018; accepted August 19, 2018)

ABSTRACT

The convective heat transfer and entropy generation of diamond-Fe_3O_4/water hybrid nanofluid through a rectangular minichannel is numerically investigated under laminar flow conditions. Nanoparticle volume fractions for diamond-Fe_3O_4/water hybrid nanofluid are in the range 0.05-0.20% and Reynolds number varies from 100 to 1000. The finite volume method is used in the numerical computation. The results obtained for diamond-Fe_3O_4/water hybrid nanofluid are compared with those of diamond/water and Fe_3O_4/water conventional nanofluids. It is found that 0.2% diamond-Fe_3O_4 hybrid nanoparticle addition to pure water provides convective heat transfer coefficient enhancement of 29.96%, at Re=1000. The results show that diamond-Fe_3O_4/water hybrid nanofluid has higher convective heat transfer coefficient and Nusselt number when compared with diamond/water and Fe_3O_4/water conventional nanofluids. For diamond-Fe_3O_4/water hybrid nanofluid, until Re=600, the lowest total entropy generation rate values are obtained for 0.20% nanoparticle volume fraction. However, after Re=800, diamond-Fe_3O_4/water hybrid nanofluid with 0.20% nanoparticle volume fraction has the highest total entropy generation rate compared to other nanoparticle volume fractions. A similar pattern emerges from the comparison with diamond/water and Fe_3O_4/water conventional nanofluids. For 0.2% nanoparticle volume fraction, diamond-Fe_3O_4/water hybrid nanofluid and diamond/water nanofluid have their minimum entropy generation rate at Re=500 and at Re=900, respectively. Moreover, this minimum entropy generation rate point changes with nanoparticle volume fraction values of nanofluids.

Keywords: Bejan number; Convective heat transfer; Entropy generation; Hybrid nanofluid; Minichannel.

NOMENCLATURE

A	area	q''	heat flux
Be	Bejan number	Re	Reynolds number
C_P	specific heat	$\dot{S}'_{gen}$	entropy generation rate per unit length
div	divergence	T	temperature
D_h	hydraulic diameter	$\vec{V}$	velocity vector
f	Darcy friction factor		
$grad$	gradient		
h	convective heat transfer coefficient	μ	dynamic viscosity
k	conductive heat transfer coefficient	ρ	density
$\dot{m}$	mass flow rate	ϕ	volumetric fraction
Nu	Nusselt number	τ	shear stress
P	Pressure	ω	coefficient defined in Eqs. (24)

1. INTRODUCTION

For today's societies and future generations all around the world, energy is the most important factor of countries' development. Decreasing conventional energy sources, based on fossil fuels, and their hazardous effect on the environment have led people either to search for new energy sources or use energy technologies more efficiently. Enhancement of heat transfer in any engineering equipment by increasing the thermal conductivity of the working fluids is one way of using energy efficiently. Nanofluid, which has been termed firstly by Choi and Eastman (Choi 1995, 1998; Eastman *et al.* 1996), is a colloidal mixture made of a base fluid, such as water, oil and ethylene glycol, and a nanoparticle with sizes under 100 nm. Various nanoparticle materials as summarized in (Lomascol 2015; Devendiran and Amirtham 2016; Adriana 2017; Nabil *et al.* 2017) have been used to obtain nanofluid. These fluids are a new generation of heat transfer fluids which can become a high potential fluid in heat transfer applications due to their ability to enhance thermal conductivity significantly.

A meaningful corpus of numerical and experimental studies has been performed for various types of nanofluids such as Al_2O_3, TiO_2, CuO, ZnO, Fe_2O_3, Fe_3O_4, Ag, carbon nanotubes (CNT), SiO_2, nanodiamond (ND) nanoparticles dispersed in water, EG and oil in both laminar and turbulent flow regimes, since the term nanofluid was first introduced by Pak and Cho (1998) for convective heat transfer. Sudarmadji *et al.* (2014) has investigated the convective heat transfer and pressure drop of nanofluid, using Al_2O_3-water nanofluid under laminar flow regime. As the development of nanofluid technology has progressed, the conventional term nanofluid has been retired recently in favor of the term "hybrid nanofluid". Hybrid nanofluids are a very new kind of nanofluids, which can be prepared by suspending different types (two or more than two) of nanoparticles in base fluid (Sarkar *et al.* 2015). Recently, various experimental and numerical studies, categorized as *i*) preparation, characterization and modelling (Suresh *et al.* 2011; Kumar *et al.* 2016; Azwadi *et al.* 2016; Sundar *et al.* 2017b) *ii*) rheological behavior (Afrand *et al.* 2016; Asadi and Asadi 2016; Zareie *et al.* 2017) *iii*) thermal conductivity (Esfe *et al.* 2015a,b; Harandi *et al.* 2016; Toghrai *et al.* 2016; Afrand 2017; Vafaei *et al.* 2017) and *iv*) convective heat transfer applications (Suresh *et al.* 2012; Madhesh *et al.* 2014; Nimmagadda and Venkatasubbaiah 2015; Azwadi and Adamu 2016; Kalidasan and Kanna 2017), have been conducted on different hybrid nanofluids by several researchers and some of these studies have been reviewed (Sarkar *et al.* 2015; Singh and Gupta 2016; Sidik *et al.* 2016; Sundar *et al.* 2017a; Leong *et al.* 2017; Minea 2017) in the available literature.

Mehrali at al. (2017) experimentally investigated the heat transfer characteristics and entropy generation rate of hybrid graphene-magnetite nanofluids under forced laminar flow conditions. In their study, the thermal characteristics of the hybrid nanofluid, compared to distilled water, consisted of an increment of 11% under magnetic field and a decrease of 41% in total entropy generation. Moghadassi *et al.* (2015) studied hybrid nanofluids numerically by using water-based Al_2O_3 and Al_2O_3-Cu hybrid nanofluid flow through a horizontal circular tube. In their study, a CFD method 0.1% volume concentration of hybrid nanofluid was used. They found that the average Nusselt number increased to 4.73% and 13.46% when the hybrid nanofluid was compared to Al_2O_3/water nanofluid and pure water, respectively. Labib *et al.* (2013) numerically investigated the laminar forced convection flow of Al_2O_3/water and Al_2O_3/ethylene glycol nanofluids. In their study, ethylene glycol base fluid was found to give better heat transfer enhancement than water. In addition, when a mixture of Al_2O_3 nanoparticles in CNTs/water nanofluids was investigated numerically, the resulting hybrid nanofluids successfully enhanced convective heat transfer. Allahyar et.al. (2016) experimentally studied the thermal performance of 97.5% alumina and 2.5% Ag hybrid nanoparticle and single type nanofluid for laminar flow conditions and 0.1-0.4 vol% nanoparticle volume fraction. The maximum rate of heat transfer was found in their study to be 31.58% higher than distilled water by using the hybrid nanofluid at a volume fraction of 0.4 vol%. Sundar et.al. (2014a) experimentally studied the convective heat transfer coefficient and friction factor for fully developed turbulent flow of MWCNT-Fe_3O_4/water hybrid nanofluids flowing through a uniformly heated circular tube at a constant heat flux. When compared with base fluid, enhancement in Nusselt number of hybrid nanofluid was found to be 31.1% for the particle loading of 3%, where Re=22000. In other study of Sundar *et al.* (2013b), thermal conductivity of ethylene glycol and water mixture based Fe_3O_4 nanofluid was investigated experimentally. Experiments were performed for different base fluids mixture with temperature ranging from 20 to 60 °C, and particle volume fraction ranging from 0.2% to 2.0%. In this study, thermal conductivity was enhanced by 46% at 2.0 vol.% of nanoparticles dispersed in 20:80% ethylene glycol and water mixture compared to other base fluids. Entropy generation analysis of graphene–alumina hybrid nanofluids under the laminar flow regime with the Reynolds number varying from 200 to 1000 was investigated by Ahammed et.al (2016) in a multiport minichannel heat exchanger. In their study, enhancement in the convective heat transfer was reported as 88.62% with decrement in total entropy generation from 0.0361 W/K to 0.0184 W/K for pure graphene–water nanofluid. Sundar *et al.* (2014b) observed 21% and 13% thermal conductivity enhancement with 3.03% weight of nanodiamond-Ni nanoparticles dispersed in water and EG respectively.

Cai *et al.* (2017) reviewed the studies about fractal-based approaches to nanofluids and nanoparticle aggregation. Xiao *et al.* (2013)

obtained an effective thermal conductivity formula for nanofluids considering the effect of Brownian motion of nanoparticles. Wei *et al.* (2016) developed a theoretical model considering two different mechanisms of heat conduction including particle aggregation and convention to investigate the effect of fractal distribution characteristics of nanoparticle aggregation on thermal conductivity of nanofluids.

Based on the available literature, to our knowledge, there are only a few papers where diamond-Fe_3O_4 hybrid nanofluids are studied. Sundar *et al.* (2016a) recently published their research on the determination of thermal conductivity and viscosity values for diamond-Fe_3O_4 hybrid nanofluids. In it, they discussed correlations. However, the convective heat transfer characteristics as well as the entropy generation of diamond-Fe_3O_4 hybrid nanofluids have never been studied. Therefore, the objective of the present investigation is to study the interrelation between the entropy generation and the convective heat transfer coefficient of diamond-Fe_3O_4 hybrid nanofluid flow through a rectangular minichannel under laminar flow regime. This numerical study encompasses different fluid types (pure water, diamond/water; Fe_3O_4/water and diamond-Fe_3O_4/water hybrid nanofluid), under constant heat flux in different Reynolds number (from Re=100 to Re=1000) and in different particle volume concentration (from 0.05% to 0.2%). The effects of pertinent parameters, such as Reynolds number and nanoparticle volume fraction, on convective heat transfer coefficient, Nusselt number, entropy generation, Bejan number of diamond-Fe_3O_4/water hybrid nanofluid are graphically examined and patterns interpreted. Moreover, results obtained for diamond-Fe_3O_4/water hybrid nanofluid are compared to those of diamond/ water and Fe_3O_4/water conventional nanofluid.

2. METHODOLOGY

2.1 Geometric Configuration

The convective heat transfer characteristics and entropy generation of diamond-Fe_3O_4/water hybrid nanofluid having different nanoparticle volume fractions through a rectangular minichannel are numerically investigated under laminar flow regime. The schematic view of the rectangular minichannel considered in this study is illustrated in Fig. 1. The height, width and length of the rectangular minichannel are assumed to be H=1.5 mm, W=1 mm and L=50 mm, respectively.

2.2 Numerical Procedure

In the present study, the single-phase approach and laminar viscous model are numerically investigated through the Finite Volume Method (FVM). ANSYS Fluent code based on the FEM method is used for numerical computations. The SIMPLE (Semi-Implicit Method for Pressure Linked Equation) algorithm (Patankar 1980) is used for dealing with the coupling between velocity and pressure. A second order upwind scheme is used to obtain higher numerical accuracy when the residual convergence criterion is less than 10^{-6} for the continuity, momentum and energy equations. In the numerical study, discretization of these governing equations refers to the Green Gauss cell-based method.

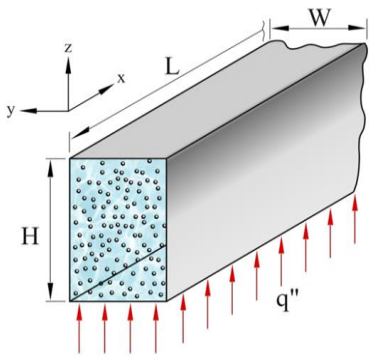

Fig. 1. Schematic view of minichannel.

2.3 Geometric Configuration

The nanofluid flow is considered under single-phase, three-dimensional, steady-state, incompressible, laminar flow conditions. The thermophysical properties of nanofluids are assumed to be temperature independent. In the view of these assumptions, the governing equations can be written as follows,

$$div(\rho\vec{V})=0 \tag{1}$$

$$div(\rho\vec{V}\vec{V})=-grad\,P+div(\mu\,grad\,\vec{V}) \tag{2}$$

$$div(\rho C_p\vec{V}T)=div(k\,grad\,T) \tag{3}$$

To be able to solve the governing equations, boundary conditions should be defined. The inlet temperature (T_{inlet}) of working fluids considered in this study is 303 K. The inlet velocities of working fluids are calculated for defined Reynolds number values by using Reynolds number formula, which is $Re=(\rho VD/\mu)$. The constant heat flux of q'' = 10000 W/m^2 is applied to the bottom surface of the minichannel. In the outlet of the minichannel, a pressure-outlet boundary condition is applied.

2.4 Thermophysical Properties of Conventional and Hybrid Nanofluids

In the solution of governing equations, the thermophysical properties of working fluids should be known. In this study, diamond-Fe_3O_4/water hybrid nanofluid and pure water is used as working fluid. Moreover, to be able to compare the results obtained for hybrid nanofluid with that of conventional nanofluids, diamond/water and Fe_3O_4/water conventional nanofluids are used.

The thermophysical properties of pure water, diamond and Fe_3O_4 nanoparticle are given in Table 1.

Table 1 Thermophysical properties of nanoparticles at 303 K (Incropera *et al.* 2006; Sundar *et al.* 2016a; Sheikholeslami and Shamlooei 2017)

Matter	ρ (kg/m^3)	Cp (J/kgK)	k (W/mK)	μ (Pas)
Pure water	995.81	4178.40	0.6172	0.000803
Diamond	3510	497.26	1000	-
Fe_3O_4	5180	670	72	-

However, the density and specific heat of diamond-Fe_3O_4 hybrid nanoparticle show variety to the degree of weight percentages of nanoparticles existing in hybrid nanoparticle. The following equations can be used to find the density and the specific heat of diamond-Fe_3O_4 hybrid nanoparticle, respectively:

$$\rho_{D-Fe_3O_4} = \frac{(\rho_D W_D)+(\rho_{Fe_3O_4} W_{Fe_3O_4})}{(W_D + W_{Fe_3O_4})} \tag{4}$$

$$Cp_{D-Fe_3O_4} = \frac{(Cp_D W_D)+(Cp_{Fe_3O_4} W_{Fe_3O_4})}{(W_D + W_{Fe_3O_4})} \tag{5}$$

In Eqs. (4) and (5), the weight percentages of diamond and Fe_3O_4 on the diamond-Fe_3O_4 hybrid nanoparticle are assumed to be 72% and 28%, respectively [42]. By using the data presented in Table 1 and Eqs. (4) and (5), the density and specific heat of diamond-Fe3O4 hybrid nanoparticle are obtained to be $\rho_{D-Fe_3O_4}$ = 3977.6 kg/m^3 and $Cp_{D-Fe_3O_4}$ = 545.58 J/kgK, respectively.

The following equations can be used to find the density and specific heat of diamond-Fe_3O_4/water hybrid nanofluid, diamond/water and Fe_3O_4/water conventional nanofluids, respectively (Das *et al.* 2008):

$$\rho_{nf} = \phi\rho_{np} + (1-\phi)\rho_{bf} \tag{6}$$

$$Cp_{nf} = \phi Cp_{np} + (1-\phi)Cp_{bf} \tag{7}$$

The thermal conductivity and viscosity of diamond-Fe_3O_4/water hybrid nanofluid can be found by applying the equations proposed by Sundar *et al.* (2016a).

Daimond-Fe_3O_4/water hybrid nanofluids:

$$k_{nf} = (a + b\phi)k_{bf} \tag{8}$$

$$\mu_{nf} = (ae^{b\phi})\mu_{bf} \tag{9}$$

where a=1.1088 and b=0.3751 in Eq. (8); a=1.368 and b=1.472 in Eq. (9) for 303 K. Equations (8) and (9) are valid with temperature ranging from 293 to 333 K and with the nanoparticle volume fractions ranging from 0.05% to 0.2%.

Sundar *et al.* (2013a; 2016b) also proposed the following equations to calculate the thermal conductivity and viscosity of diamond/water and Fe_3O_4/water nanofluids.

Diamond/water nanofluid:

$$k_{nf} = 1.041k_{bf}\left[(1+\phi)^{0.22}\left(\frac{T_{min}}{T_{max}}\right)^{0.0539}\right] \tag{10}$$

$$\mu_{nf} = 1.097\mu_{bf}\left[(1+\phi)^{0.632}\left(\frac{T_{min}}{T_{max}}\right)^{0.056}\right] \tag{11}$$

where T_{min}=293 K and T_{max}=333 K. Equations (10) and (11) are valid for nanoparticle volume fractions from 0.0% to 1.0%.

Fe_3O_4/water nanofluids:

$$k_{nf} = k_{bf}(1+10.5\phi)^{0.1051} \tag{12}$$

$$\mu_{nf} = \mu_{bf}\left(1+\frac{\phi}{12.5}\right)^{6.356} \tag{13}$$

where Eqs. (12) and (13) can be used with the nanoparticle volume fraction ranging from 0.0% to 1.0%.

The average convective heat transfer and average Nusselt number is calculated by using the following equations:

$$h = \frac{q''}{(T_w - T_f)} \tag{14}$$

$$Nu = \frac{hD}{k} \tag{15}$$

The average Darcy friction factor of flow can be determined by using the following equation:

$$f = 2\frac{D}{L}\frac{\Delta P}{\rho V^2} \tag{16}$$

Entropy is defined as the measure of molecular disorder and randomness. The total entropy generation rate per unit length for internal flow is expressed as follows:

$$\dot{S}'_{gen,total} = \dot{S}'_{gen,heat\ transfer} + \dot{S}'_{gen,\ fluid\ friction} \tag{17}$$

The first term on the right side of Eq. (17) is entropy generation rate due to heat transfer per unit length, while the second term is entropy generation rate due to fluid fraction per unit length. The following equations can be used to express entropy generation rates due to heat transfer and to fluid friction per unit length, respectively:

$$\dot{S}'_{gen,heat\ transfer} = \frac{q''^2\pi D^2}{kT_b^{\ 2}Nu} \tag{18}$$

$$\dot{S}'_{gen,\ fluid\ friction} = \frac{8\dot{m}^3}{\pi^2\rho^2T_b}\frac{f}{D^5} \tag{19}$$

where $\dot{m} = \rho AV$ is the mass flow rate, and $T_b = (T_{in} + T_{out})/2$ is the bulk temperature of fluid. Bejan number is formulated as follows:

$$Be = \frac{\dot{S}'_{gen,heat\ transfer}}{\dot{S}'_{gen,total}} \tag{20}$$

and it is defined as the ratio of entropy generation rate due to heat transfer to total entropy generation rate.

2.5 Grid Independence and Code Validation

The mesh independency test is carried out to eliminate the effect of grid number on the numerical computation results. The results of mesh independency test are shown in Table 2. To carry out the solutions, the 24*36*600 mesh model is selected. The accuracy of the selected model is tested by comparing its results with those of Ho and Chen (2013) and of Moraveji and Ardehali (2013). Figure 2 illustrates comparisons. The average deviations between the results of present study and the results of Ho and Chen (2013) and Moraveji and Ardehali (2013) are 4.8% and 3.99%, respectively.

Table 2 The mesh independency test

Mesh	*Nu*	*f*	*ΔNu (%)*	*Δf (%)*
6*8*600	8.7150	0.08465	-	-
10*15*600	8.7992	0.08617	0.97	1.79
12*18*600	8.8246	0.08728	0.29	1.29
18*24*600	8.6530	0.08907	-1.94	2.04
24*36*600	8.5987	0.09021	-0.63	1.28

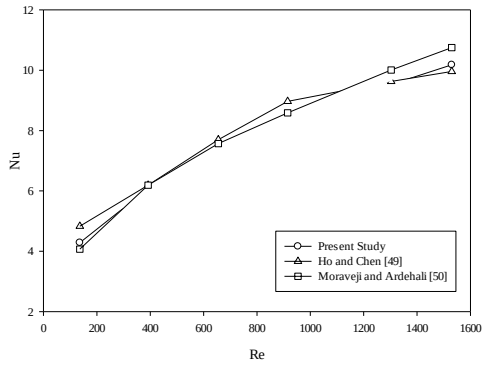

Fig. 2. The model accuracy test.

3. RESULT AND DISCUSSIONS

The convective heat transfer characteristics and entropy generation of diamond-Fe_3O_4 hybrid nanofluid through a rectangular minichannel are numerically investigated under laminar flow regime. In the analysis, different nanoparticle volume fractions (ϕ = 0.05-0.2%) of diamond-Fe_3O_4 hybrid nanofluid are used. Reynolds number is in the range of 100 and 1000, and constant heat flux of 10000 W/m^2 is applied to bottom surface of the minichannel. The results obtained for diamond-Fe_3O_4 hybrid nanofluid are presented in this section. Moreover, the results are compared with those of diamond/water and Fe_3O_4/water conventional nanofluids.

3.1 Convective Heat Transfer Coefficient

The convective heat transfer coefficient of diamond-Fe_3O_4 hybrid nanofluid is obtained by using Eq. (14) and results are presented in Fig. 3.

As can be seen from Fig. 3, the convective heat transfer coefficient increases with an increase in nanoparticle volume fraction of hybrid nanofluid. The maximum convective heat transfer coefficient enhancement is 29.96% for diamond-Fe_3O_4 hybrid nanofluid having 0.2% nanoparticle volume fraction at Re=1000.

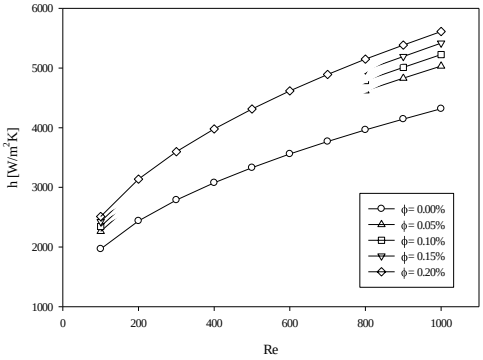

Fig. 3. The convective heat transfer coefficients for diamond-Fe_3O_4/water hybrid nanofluid.

Figure 4 shows the comparison of convective heat transfer values obtained for diamond-Fe_3O_4/water hybrid nanofluid with that of diamond/water and Fe_3O_4/water conventional nanofluids for 0.2% nanoparticle volume fraction.

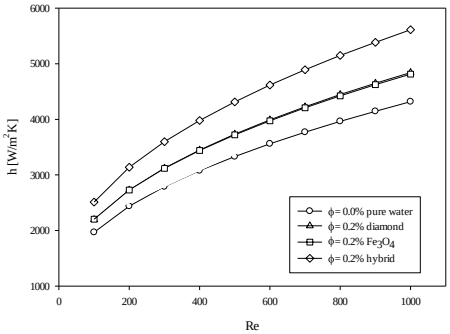

Fig. 4. The comparison of convective heat transfer coefficients for conventional and hybrid nanofluids.

The convective heat transfer coefficients obtained for diamond-Fe_3O_4/water hybrid nanofluid are higher than those of diamond/water and Fe_3O_4/water nanofluids. Almost the same convective heat transfer coefficients are obtained for diamond/water and Fe_3O_4/water nanofluids. At Re=1000, the convective heat coefficient values obtained for diamond-Fe_3O_4/water hybrid nanofluid and diamond/water and Fe_3O_4/water conventional nanofluids are 5613.20 W/m^{2}K, 4842.49 W/m^{2}K, and 4813.77 W/m^{2}K, respectively. This means that the convective heat transfer coefficient obtained for diamond-Fe_3O_4/water hybrid nanofluid is 15.91% higher than that of diamond/water nanofluid as well as 16.61% higher than that of Fe_3O_4/water nanofluid. The smallest temperature difference

between wall temperature and bulk temperature obtained for diamond-Fe_3O_4/water hybrid nanofluid. Moreover, in analysis for fixed Reynolds number, the highest flow velocity value is obtained for diamond-Fe_3O_4/water hybrid nanofluid. These parameters cause to that diamond-Fe_3O_4/water hybrid nanofluid has the highest convective heat transfer coefficient.

3.2 Nusselt Number

The Nusselt number of diamond-Fe_3O_4/water hybrid nanofluid can be calculated with Eq. (16). The results obtained for diamond-Fe_3O_4/water hybrid nanofluid are illustrated in Fig. 5 and the results are compared with those of diamond/water and Fe_3O_4/water nanofluid in Fig. 6.

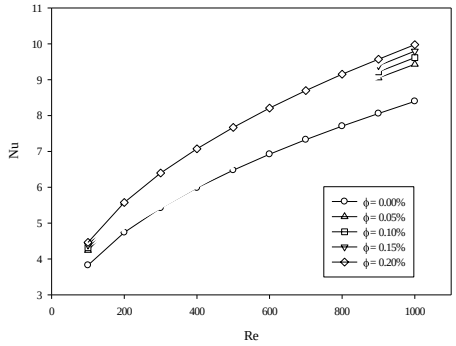

Fig. 5. The Nusselt number for diamond-Fe_3O_4/water hybrid nanofluid.

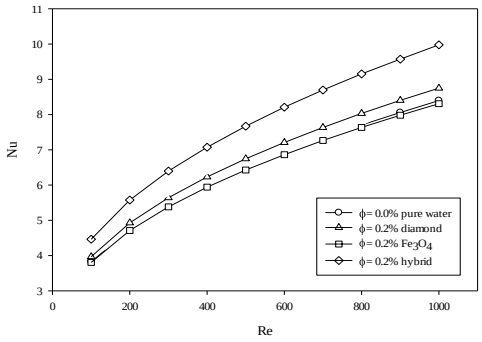

Fig. 6. The comparison of Nusselt numbers for conventional and hybrid nanofluids.

The Nusselt number increases with increasing nanoparticle volume fraction of diamond-Fe_3O_4/water hybrid nanofluid. In diamond-Fe_3O_4/water hybrid nanoparticle, the addition of 0.2%, at Re=1000, renders the Nusselt number 18.82% higher than that of pure water.

The highest Nusselt number values are obtained for diamond-Fe_3O_4/water hybrid nanofluid, followed by diamond/water nanofluid, pure water and Fe_3O_4/water nanofluid, respectively. The reason behind the Nusselt number for Fe_3O_4 nanofluid, which is lower than the number for pure water, is that the increment existing in thermal conductivity coefficient with Fe_3O_4 nanofluid is higher than that of the convective heat transfer coefficient. At Re=1000, the highest and the lowest Nusselt numbers are Nu=9.98 and Nu=8.31 for diamond-Fe_3O_4 hybrid nanofluid and Fe_3O_4 nanofluid, respectively. At Re=1000, Nusselt number values obtained for diamond nanofluid and pure water are also Nu=8.75 and Nu=8.40, respectively.

According to Figs. 4 and 6, it is clear that diamond-Fe_3O_4/water hybrid nanofluid exhibits higher thermal performance than pure water, diamond/water and Fe_3O_4/water conventional nanofluids.

3.3 Pressure Drop

The pressure drop values obtained with numerical computations for diamond-Fe_3O_4/water hybrid nanofluid are illustrated in Fig. 7.

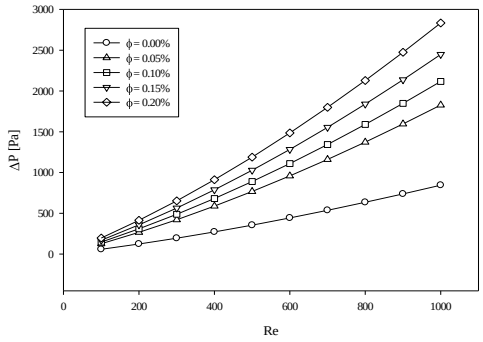

Fig. 7. The pressure drop for diamond-Fe_3O_4/water hybrid nanofluid.

Diamond-Fe_3O_4/water hybrid nanoparticle addition to pure water causes an extreme increment in pressure drop of flow. The maximum pressure drop values are obtained for diamond-Fe_3O_4/water hybrid nanofluid having 0.2% nanoparticle volume fraction. In Re=1000, the pressure drop of flow increases from 845.08 Pa to 2834.31 Pa with 0.2% diamond-Fe_3O_4 hybrid nanoparticle addition to pure water.

Figure 8 shows the comparison of pressure values of diamond-Fe_3O_4/water hybrid nanofluid with that of diamond/water and Fe_3O_4/water conventional nanofluids.

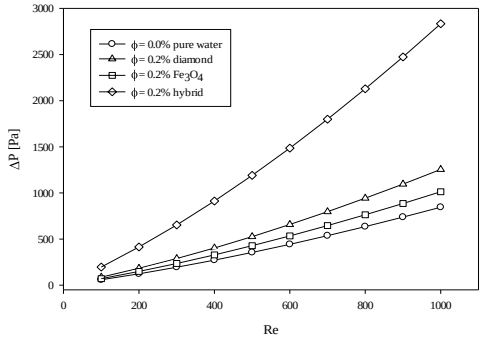

Fig. 8. The comparison of pressure drop for conventional and hybrid nanofluids.

The pressure drop of diamond-Fe_3O_4/water hybrid

nanofluid is much more than that of diamond/water and Fe_3O_4/water conventional nanofluids. Moreover, the incremental trend in pressure drop of diamond-Fe_3O_4/water hybrid nanofluid is also higher than that of others. This outcome is due to the higher viscosity values of diamond-Fe_3O_4/water hybrid nanofluid. At Re=1000, the pressure drop values for diamond-Fe_3O_4/water hybrid nanofluid, diamond/water nanofluid, Fe_3O_4/water nanofluid, and pure water are 2834.31 Pa, 1254.86 Pa, 1013.09 Pa and 845.08 Pa, respectively.

3.4 Darcy Friction Factor

The Darcy friction factor of diamond-Fe_3O_4/water hybrid nanofluid is obtained by using Eq. (16). Darcy friction factor values obtained for diamond-Fe_3O_4/water hybrid nanofluid are shown in Fig. 9 and are compared with those of diamond/water and Fe_3O_4/water conventional nanofluids in Fig. 10.

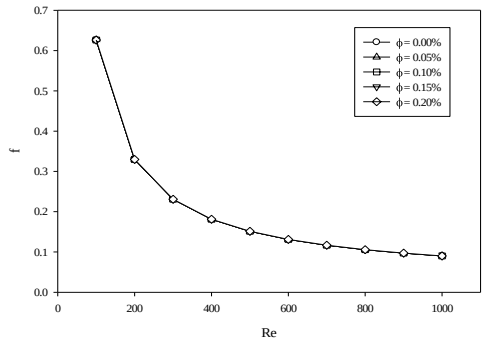

Fig. 9. The Darcy friction factor for diamond-Fe_3O_4/water hybrid nanofluid.

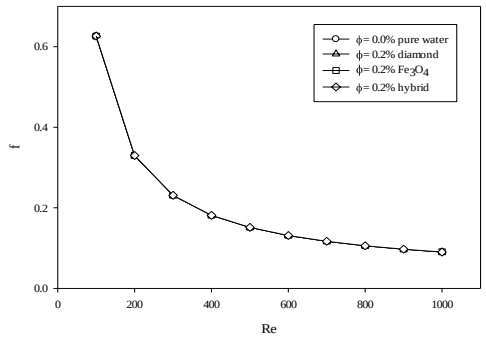

Fig. 10. The comparison of Darcy friction factor for conventional and hybrid nanofluids.

Although the hybrid nanoparticle addition to pure water increases pressure drop of flow, the Darcy friction factor is not affected by it. As can be seen from Figs. 9 and 10, the same Darcy friction factor values are obtained for all working fluids considered in this study. Either hybrid or conventional nanoparticle addition to pure water increases pressure drop; however, at the same time, it also increases the flow velocity for defined Reynolds number values. Thus, the dimensionless pressure drop is not affected by either hybrid or conventional nanoparticle addition to pure water even though pressure drop is affected by it.

3.5 Entropy Generation Rate

As mentioned in section 2.4, the entropy generation rate of internal flow results from the heat transfer and the fluid friction between channel wall and working fluid. The entropy generation rate due to heat transfer per unit length for diamond-Fe_3O_4/water hybrid nanofluid is calculated with Eq. (18) and is illustrated in Fig. 11.

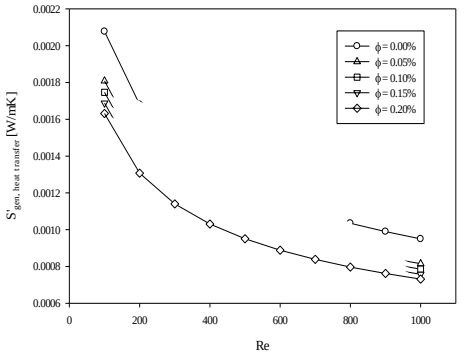

Fig. 11. The entropy generation rate due to heat transfer for diamond-Fe_3O_4/water hybrid nanofluid.

Figure 11 clearly shows that the entropy generation rate due to heat transfer per unit length decreases with increasing nanoparticle volume fraction of diamond-Fe_3O_4/water hybrid nanofluid. The minimum entropy generation rate due to heat transfer is obtained for diamond-Fe_3O_4/water hybrid nanofluid having 0.2% nanoparticle volume fraction. This phenomenon is due to diamond-Fe_3O hybrid nanoparticle addition to pure water which increases thermal conductivity coefficient and Nusselt number. Therefore, diamond-Fe_3O_4 hybrid nanoparticle addition to pure water causes a reduction in entropy generation due to heat transfer even though it decreases nanofluid bulk temperature. The magnitude of the reduction is 21.45% and 23.04% for diamond-Fe_3O_4 hybrid nanofluid having 0.2% nanoparticle volume fraction at Re=100 and Re=1000, respectively. In addition, the entropy generation rate due to heat transfer decreases with increasing Reynolds numbers. This phenomenon is due to an increase in the Reynolds number which leads to an increase in the Nusselt number.

The comparison of the entropy generation rate due to heat transfer of a diamond-Fe_3O_4/water hybrid nanofluid with that of a diamond/water and Fe_3O_4/water conventional nanofluids is shown in Fig. 12.

As can be seen from Fig. 12, the diamond-Fe_3O_4/water hybrid nanofluid has a lower entropy generation rate than others due to heat transfer. The obtained values for entropy generation rate due to heat transfer of diamond/water and Fe_3O_4/water conventional nanofluids are almost the same. At Re=100, the obtained results are 0.001632 W/mK, 0.001863 W/mK and 0.001856 W/mK for diamond-Fe_3O_4/water hybrid nanofluid, diamond/water, and

Fe_3O_4/water nanofluid, respectively. The main parameter causes to the smallest entropy generation rate due to heat transfer for diamond-Fe_3O_4/water hybrid nanofluid compared to other nanofluids considered in this study is Nusselt number. The highest Nusselt values obtained for diamond-Fe_3O_4/water hybrid nanofluid cause to the smallest entropy generation rate due to heat transfer.

The entropy generation rate due to fluid friction per unit length for diamond-Fe_3O_4/water hybrid nanofluid is calculated with Eq. (19) and the obtained results are shown in Fig. 13.

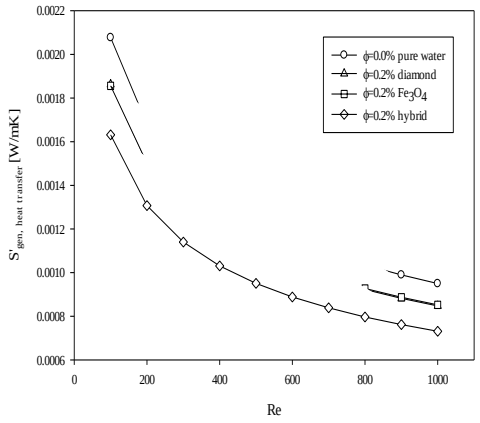

Fig. 12. The comparison of entropy generation rate due to heat transfer for conventional and hybrid nanofluids.

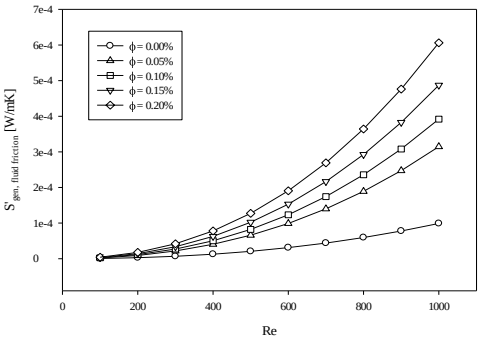

Fig. 13. The entropy generation rate due to fluid friction for diamond-Fe_3O_4/water hybrid nanofluid.

As can be seen from Fig. 13, contrary to the entropy generation due to heat transfer, the entropy generation due to fluid friction per unit length greatly increases with increases in the nanoparticle volume fraction of diamond-Fe_3O_4/water hybrid nanofluid. At Re=100 and Re=1000, for diamond-Fe_3O_4/water hybrid nanofluid having 0.2% nanoparticle volume fraction, the entropy generation rates due to fluid fraction per unit length are 4.2045×10^{-6} W/mK and 6.0623×10^{-4} W/mK, respectively. This pattern illustrates that the entropy generation due to fluid friction per unit length for diamond-Fe_3O_4/water hybrid nanofluid increases greatly with increases in the Reynolds number.

The diamond-Fe_3O_4 hybrid nanoparticle addition to pure water increases the fluid density and viscosity. In consideration of defined Reynolds number values, a higher increment in viscosity compared to density causes an increment in flow velocity. Therefore, extreme increments in entropy generation due to fluid friction mainly result from velocity increments.

Figure 14 shows the comparison of entropy generation rate due to fluid friction per unit length of diamond-Fe_3O_4/water hybrid nanofluid with that of diamond/water and Fe_3O_4/water conventional nanofluids.

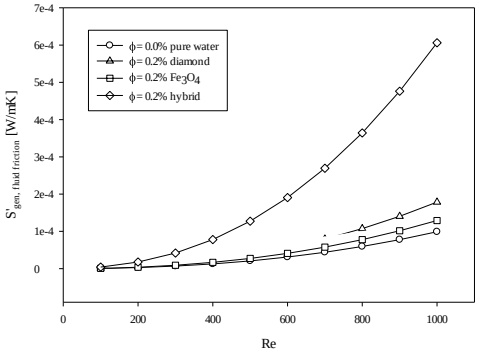

Fig. 14. The comparison of entropy generation rate due to fluid friction for conventional and hybrid nanofluids.

It can be clearly seen from Fig. 14 that the highest entropy generation rate due to fluid friction is belonging to diamond-Fe_3O_4/water hybrid nanofluid. At Re=1000, the entropy generation rates due to fluid friction for diamond/water and Fe_3O_4/water nanofluids are 1.7867×10^{-4} W/mK and 1.2898×10^{-4} W/mK, respectively, whereas the entropy generation rate is 6.0623×10^{-4} W/mK for a diamond-Fe_3O_4/water hybrid nanofluid. In comparison for fixed Reynolds number, the highest flow velocity is obtained for diamond-Fe_3O_4/water hybrid nanofluid due to it's the highest viscosity value. The highest flow velocity causes to the highest entropy generation rate due to fluid friction.

The total entropy generation rate per unit length for diamond-Fe_3O_4/water hybrid nanofluid is found with Eq. (17) and results are illustrated in Fig. 15.

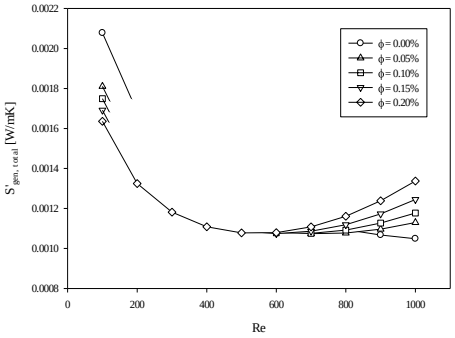

Fig. 15. The total entropy generation rate for diamond-Fe_3O_4/water hybrid nanofluid.

As can be seen from Fig. 15, the total entropy generation rate values per unit length of diamond-Fe_3O_4/water hybrid nanofluids decrease until a defined Reynolds number and then start to increase again, while values for pure water consistently decrease until Re=1000. For Re<500, the total entropy generation rate decreases with increasing nanoparticle fraction. For Re<700, the highest total entropy generation rate per unit length is obtained for pure water. Until Re=600, the lowest total entropy generation rate per unit length is observed for diamond-Fe_3O_4/water hybrid nanofluid having 0.2% nanoparticle volume fraction. In Re=600, almost the same values are obtained for all considered nanoparticle volume fractions of diamond-Fe_3O_4/water hybrid nanofluid. For $Re \geq 900$, contrary to the pattern exhibited at Re<500, the total entropy generation rate per unit length increases with increments of the nanoparticle volume fraction of diamond-Fe_3O_4/water hybrid nanofluid. The highest total entropy generation rate is obtained for diamond-Fe_3O_4/water hybrid nanofluid having 0.2% nanoparticle volume fraction after Re=800, while the lowest one is obtained for pure water after Re=900. Moreover, it is observed that diamond-Fe_3O_4/water hybrid nanofluid having 0.2% nanoparticle volume fraction has its minimum total entropy generation rate at Re=500. However, this minimum entropy generation rate is observed at Re=600 for nanoparticle volume fraction of 0.15%, while it is observed at Re=700 for nanoparticle volume fraction of 0.10% and 0.05%. The incremental tendency in total entropy generation rate of diamond-Fe_3O_4/water hybrid nanofluid after a defined Reynolds number results from an extreme increment in the entropy generation rate due to fluid friction of diamond-Fe_3O_4 hybrid nanofluid with increasing Reynolds numbers and nanoparticle volume fractions.

xThe comparison of the total entropy generation rate per unit length of a diamond-Fe_3O_4/water hybrid nanofluid with that of diamond/water and Fe_3O_4/water conventional nanofluids is illustrated in Fig. 16.

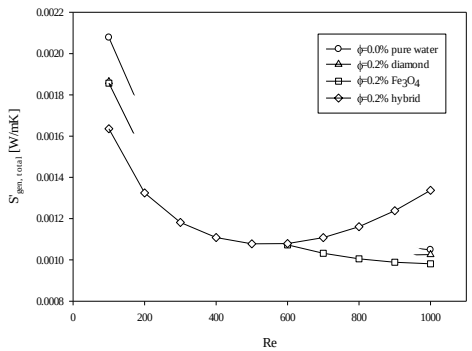

Fig. 16. The comparison of total entropy generation rate for conventional and hybrid nanofluids.

Until Re=600, diamond-Fe_3O_4/water hybrid nanofluid has the lowest total entropy generation rate, while pure water has the highest one. Moreover, until Re=500, almost the same values are obtained for diamond/water and Fe_3O_4/water conventional nanofluids. At Re=600, all working nanofluids considered in this study (except pure water) have almost the same entropy generation rate. After Re=800, the highest entropy generation rate is obtained for diamond-Fe_3O_4/water hybrid nanofluid and it is followed by pure water, diamond/water and Fe_3O_4/water conventional nanofluid, respectively. It is also found that the minimum entropy generation rate for diamond-Fe_3O_4/water hybrid nanofluid is obtained at Re=500, whereas diamond/water nanofluid has its minimum entropy generation rate at Re=900. After these Reynolds numbers, diamond-Fe_3O_4/water hybrid nanofluid and diamond/water nanofluid show increasing entropy generation rates. A similar pattern may be obtained for Fe_3O_4/water nanofluid with extends Reynolds number interval. Because decreasing entropy generation rates of Fe_3O_4/water nanofluid are accompanied by deceleration at higher Reynolds numbers, rates are much greater at lower Reynolds numbers.

As can be seen from Figs. 12 and 14, the entropy generation rate due to heat transfer decreases with increase in Reynolds number, while entropy generation due to fluid friction increases with increase in Reynolds number. Until a Reynolds number, the decrement in entropy generation is dominant. After this Reynolds number, the increment in entropy generation rate due to fluid friction prevails to the decrement in entropy generation due to heat transfer. Therefore, total entropy generation rate decreases until a Reynolds number, and then increases. This trend can clearly be seen from Fig. 17 for diamond-Fe_3O_4/water hybrid nanofluid. Similar trend may be observed for diamond/water and Fe_3O_4/water nanofluids for higher Reynolds number values than Re=1000. Because, slope of total entropy generation rate for diamond/water and Fe_3O_4/water nanofluids decreases with Reynolds number values approaching to Re=1000.

3.6 Bejan Number

Bejan number of diamond-Fe_3O_4/water hybrid nanofluid is calculated by using Eq. (20). The results obtained for diamond-Fe_3O_4/water hybrid nanofluid and their comparison with those of diamond/water and Fe_3O_4/water conventional nanofluids are shown in Figs. 17 and 18, respectively.

It is found that Bejan number values of pure water and all considered nanoparticle volume fractions of diamond-Fe_3O_4/water hybrid nanofluid are almost equal to unity at Re=100. This means that almost all of total entropy generation is due to heat transfer. Bejan number decreases with increasing Reynolds number. This trend shows that the contribution of entropy generation resulting from heat transfer to total entropy generation decreases with increasing Reynolds numbers. In other words, the contribution of entropy generation due to fluid friction to total entropy generation increases with increasing Reynolds numbers. Moreover, decreases in Bejan number values with increasing Reynolds numbers

for diamond-Fe_3O_4/water hybrid nanofluid are higher compared to those of pure water.

As can be seen from Fig. 18, diamond-Fe_3O_4/water hybrid nanofluid has the lowest Bejan number values. At Re=1000, Bejan number values of diamond-Fe_3O_4/water hybrid nanofluid, diamond/water nanofluid, Fe_3O_4/water nanofluid and pure water are 0.55, 0.83, 0.87 and 0.91, respectively. This means that entropy generation due to fluid friction can be dominant at lower Reynolds numbers for diamond-Fe_3O_4/water hybrid nanofluid compared to that of diamond/water and Fe_3O_4/water nanofluid.

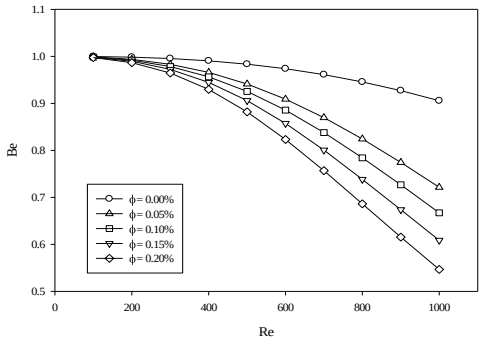

Fig. 17. The Bejan number for diamond-Fe_3O_4/water hybrid nanofluid.

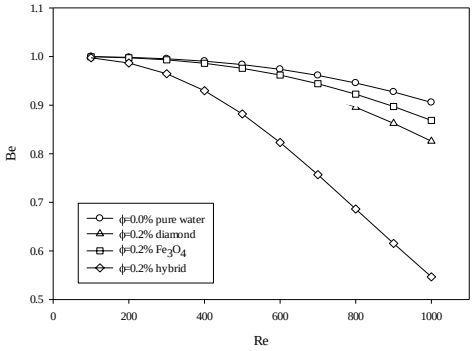

Fig. 18. The comparison of Bejan number for conventional and hybrid nanofluids.

4. CONCLUSION

In this study, laminar forced convection and entropy generation rate of diamond-Fe_3O_4/water hybrid nanofluid through a rectangular minichannel were numerically investigated for different nanoparticle volume fractions. In addition, results obtained for diamond-Fe_3O_4/water hybrid nanofluid were compared with those of diamond/water and Fe_3O_4/water conventional nanofluids. Diamond-Fe_3O_4/water hybrid nanofluid was found to have the highest convective heat transfer coefficient and Nusselt number. However, the highest pressure drop values were also obtained for diamond-Fe_3O_4/water hybrid nanofluid. Future studies should be focused on the pressure drop or viscosity reduction of diamond-Fe_3O_4/water hybrid nanofluid.

In the present study, the entropy generation rate analysis showed that the gradation of hybrid and conventional nanofluids changed with Reynolds numbers. For nanoparticle volume of 0.2%, diamond-Fe_3O_4/water hybrid nanofluid had the highest entropy generation rate between 100<Re<600, while it had the lowest one between 800<Re<1000 compared to others. Moreover, minimum entropy generation rates were found for hybrid and conventional nanofluids. Diamond-Fe_3O_4/water hybrid nanofluid having nanoparticle volume fractions of 0.05%, 0.10%, 0.15% and 0.20% had its minimum entropy generation rate values at Re=700, Re=700, Re=600 and Re=500, respectively. In a similar manner, diamond/water nanofluid had its minimum entropy generation rate at Re=900. To be able to determine the minimum entropy generation rate point of Fe_3O_4/water nanofluid, future analyses should be realized in a larger Reynolds number interval. Although this minimum entropy generation rate is related to the thermophysical properties of nanofluids, it is also affected by the hydraulic diameter of investigated channel. It is well known that the entropy generation rate due to fluid friction is a dominant property of microchannels precisely because of their very small hydraulic diameters (Sohel *et al.* 2013). Thus, results may be different in conventional channels. It is our intention to continue to investigate the minimum entropy generation rate in future studies.

REFERENCES

Adriana, M. A. (2017). Hybrid nanofluids based on Al_2O_3, TiO_2 and SiO_2: Numerical evaluation of different approaches. *Inter. J. of Heat and Mass Transf.* 104, 852-860.

Afrand, M. (2017). Experimental study on thermal conductivity of ethylene glycol containing hybrid nano-additives and development of a new correlation. *App. Thermal Eng.* 110, 1111-1119.

Afrand, M., D. Toghraie and B. Ruhani (2016). Effects of temperature and nanoparticles concentration on rheological behaviour of Fe_3O_4–Ag/EG hybrid nanofluid: An experimental study. *Exp. Therm.and Fluid Sci.* 77, 38-44.

Ahammed, N., L. G. Asirvatham and S. Wongwises (2016). Entropy generation analysis of graphene-alumina hybrid nanofluid in multiport minichannel heat exchanger coupled with thermoelectric cooler. *Inter. J. of Heat and Mass Transf.* 103, 1084-1097.

Allahyar, H. R., F. Hormozi and B. Zarenezhad (2016). Experimental investigation on the thermal performance of a coiled heat exchanger using a new hybrid nanofluid. *Exp. Therm. and Fluid Sci.* 76, 324-329.

Asadi, M. and A. Asadi (2016). Dynamic viscosity of MWCNT/ZnO–engine oil hybrid nanofluid: An experimental investigation and new correlation in different temperatures and solid concentrations. *Int. Commun. in Heat and Mass Transf.* 76, 41-45.

Azwadi, C. S. N. and I. M. Adamu (2016). Turbulent force convective heat transfer of hybrid nano fluid in a circular channel with constant heat flux. *J. of Advanced Res. in Fluid Mech. and Thermal Sci.* 19, 1-9.

Azwadi, C. S. N., I. M. Adamu and M. M. Jamil (2016). Preparation methods and thermal performance of hybrid nanofluids. *J. of Adv. Review on Sci. Res.* 24, 13-23.

Cai, J., X. Hu, B. Xiao, Y. Zhou and W. Wei (2017). Recent developments on fractal-based approaches to nanofluids and nanoparticle aggregation. *Inter. J. of Heat and Mass Transfer* 105, 623-637.

Choi, S. U. S. (1995). Enhancing thermal conductivity of fluids with nanoparticles, developments and applications of non-Newtonian flows. *ASME 231*, 99-105.

Choi, S. U. S. (1998). Nanofluid technology: current status and future research. *Korea-U S. Technical Conference on Strategic Technologies*, Vienna, VA.

Das, S. K., S. U. S. Choi, W. Yu and T. Pradeep (2008). *Nanofluids Science and Technology*. John Wiley and Sons.

Devendiran, D. K. and V. A. Amirtham (2016). A review on preparation, characterization, properties and applications of nanofluids. *Renew. and Sustain. Energy Reviews* 60, 21-40.

Eastman, J. A., S. U. S. Choi, S. Li, L. J. Thompson and S. Lee (1996). Enhanced thermal conductivity through the development of nanofluids. *Fall Meeting of the Materials Research Society (MRS)*, Boston, USA.

Esfe, M. H., A. A. A. Arani, M. Rezaie, M. W. Yan and A. Karimipour (2015a). Experimental determination of thermal conductivity and dynamic viscosity of Ag–MgO/water hybrid nanofluid. *Inter. Commun. in Heat and Mass Transf.* 66, 189-195.

Esfe, M. H., S. Wongwises, A. Naderi, A. Asadi, M. R. Safaei, H. Rostamian, M. Dahari and A. Karimipour (2015b). Thermal conductivity of Cu/TiO_2–water/EG hybrid nanofluid: Experimental data and modelling using artificial neural network and correlation. *Inter. Commun. in Heat and Mass Transf.* 66, 100-104.

Harandi, S. S., A. Karimipour, M. Afrand, M. Akbari and A. D'Orazio (2016). An experimental study on thermal conductivity of F-MWCNTs–Fe3O4/EG hybrid nanofluid: Effects of temperature and concentration. *Inter. Commun. in Heat and Mass Transf.* 76, 171-177.

Ho, C. J. and W. C. Chen (2013). An experimental study on thermal performance of Al_2O_3/water nanofluid in a minichannel heat sink. *App. Therm. Eng.* 50, 516-522.

Incropera, F. P, D. P. DeWitt, T. L. Bergman and A. S. Lavine (2006). *Introduction to Heat Transfer*. John Wiley and Sons.

Kalidasan, K. and P. R. Kanna (2017). Natural convection on an open square cavity containing diagonally placed heaters and adiabatic square block and filled with hybrid nanofluid of nanodiamond-cobalt oxide/water. *Inter. Commun. in Heat and Mass Transf.* 81, 64-71.

Kumar, M. S., V. Vasu and A. V. Gopal (2016). Thermal conductivity and rheological studies for Cu–Zn hybrid nanofluids with various base fluids. *J. of the Taiwan Inst. of Chem. Eng.* 66, 321-327.

Labib, M. N., M. J. Nine, H. Afrianto, H. Chung and H. Jeong (2013). Numerical investigation on effect of base fluids and hybrid nanofluid in forced convective heat transfer. *Inter. J. of Therm. Sci.* 71, 163-171.

Leong, K. Y., K. Z. K. Ahmad, H. C. Ong, M. C. Ghazali and A. Baharum (2017). Synthesis and thermal conductivity characteristic of hybrid nanofluids – A review. *Renew. and Sustain. Energy Reviews* 75, 868-878.

Lomascol, M., G. Colangel, M. Milanese and A. Risi (2015). Review of heat transfer in nanofluids: conductive, convective and radiative experimental results. *Renew. and Sustain. Energy Reviews* 43, 1182-1198.

Madhesh, D., R. Parameshwaran and S. Kalaiselvan (2014). Experimental investigation on convective heat transfer and rheological characteristics of Cu-TiO_2 hybrid nanofluids. *Exp. Thermal and Fluid Sci.* 52, 104-115.

Mehrali, M., E. Sadeghinezhad, A. R. Akhiani, S. T. Latibari, H. S. C. Metselaar, A. Sh. Kherbeet and M. Mehrali (2017). Heat transfer and entropy generation analysis of hybrid graphene/Fe_3O_4 ferro-nanofluid flow under the influence of a magnetic field. *Powder Techn*. 308, 149-157.

Minea, A. A. (2017). Challenges in hybrid nanofluids behavior in turbulent flow: Recent research and numerical comparison. *Renew. and Sustain. Energy Reviews* 71, 426-434.

Moghadassi, A., E. Ghomi and F. Parvizian (2015). A numerical study of water based Al2O3 and Al2O3-Cu hybrid nanofluid effect on forced convective heat transfer. *Inter. J. of Thermal Sci.* 92, 50-57.

Moraveji, M. K. and R. M. Ardehali (2013). CFD modelling (comparing single and two phase approaches) on thermal performance of Al_2O_3/water nanofluid in minichannel heat sink. *Inter. Commun. in Heat and Mass Transf.* 44, 157-164.

Nabil, M. F., W. H. Azmi, K. A. Hamid, N. N. M. Zawawi, G. Priyandoko and R. Mamat (2017). Thermo-physical properties of hybrid

nanofluids and hybrid nanolubricants: A comprehensive review on performance. *Inter. Commun. in Heat and Mass Transf.* 83, 30-39.

Nimmagada, R. and K. Venkatasubbaiah (2015). Conjugate heat transfer analysis of micro-channel using novel hybrid nanofluids (Al_2O_3 + Ag/Water). *Europ. J. of Mech. B/Fluids* 52, 19-27.

Pak, B. C. and Y. Cho (1998). Hydrodynamic and heat transfer study of dispersed fluids with submicron metallic oxide particle. *Exp Heat Transf* 11, 151-170.

Patankar, S. V. (1980). *Numerical Heat Transfer and Fluid Flow*. CRC Press.

Sarkar, J., P. Ghosh and A. Adil (2015). A review on hybrid nanofluids: Recent research, development and applications. *Renew. and Sustain. Energy Reviews* 43, 164-177.

Sheikholeslami, M. and M. Shamlooei (2017). Fe_3O_4-H_2O nanofluid natural convection in presence of thermal radiation. *Inter. J. of Hydrogen Energy* 42, 5708-5718.

Sidik, N. A. C., I. M. Adamu, M. M. Jamil, G. H. R. Kefayati, R. Mamat and G. Najati (2016). Recent progress on hybrid nanofluids in heat transfer applications: A comprehensive review. *Inter. Commun. in Heat and Mass Transf.* 78, 68-79.

Singh, V. and M. Gupta (2016). Heat transfer augmentation in a tube using nanofluids under constant heat flux boundary condition: A review. *Energy Conv. and Management* 123, 290-307.

Sohel, M. R., R. Saidur, N. H. Hassan, M. M. Elias, S. S. Khaleduzzaman and I. M. Mahbubul (2013). Analysis of entropy generation using nanofluid flow through the circular microchannel and minichannel heat sink. *Inter. Commun. in Heat and Mass Transf.* 46, 85-91.

Sudarmadji, S., S. Soeparman, S. Wahyudi and N. Hamidy (2014). Effects of cooling process of Al_2O_3-water nanofluid on convective heat transfer. *FME Transactions* 42, 155-161.

Sundar, L. S., E. V. Ramana, M. P. F. Graca, M. K. Singh and A. C. M. Sousa (2016a). Nanodiamond-Fe3O4 nanofluids: Preparation and measurement of viscosity, electrical and thermal conductivities. *Inter. Commun. in Heat and Mass Transf.* 73, 62-74.

Sundar, L. S., K. V. Sharma, M. K. Singh and A. C. M. Sousa (2017a). Hybrid nanofluids preparation, thermal properties, heat transfer and friction factor - A review. *Renew. and Sustain. Energy Reviews* 68, 185-198.

Sundar, L. S., M. J. Hortiguela, M. K. Singh and A. C. M. Sousa (2016b). Thermal conductivity and viscosity of water based nanodiamond (ND) nanofluids: An experimental study. *Inter. Commun. in Heat and Mass Transf.* 76, 245-255.

Sundar, L. S., M. K. Singh and A. C. M. Sousa (2013a). Investigation of thermal conductivity and viscosity of Fe3O4 nanofluid for heat transfer applications. *Inter. Commun. in Heat and Mass Transf.* 44, 7-14.

Sundar, L. S., M. K. Singh and A. C. M. Sousa (2013b). Thermal conductivity of ethylene glycol and water mixture based Fe_3O_4 nanofluid. *Inter. Commun. in Heat and Mass Transf.* 49, 17-24.

Sundar, L. S., M. K. Singh and A. C. M. Sousa (2014a). Enhanced heat transfer and friction factor of MWCNT–Fe_3O_4/water hybrid nanofluids. *Inter. Commun. in Heat and Mass Transf.* 52, 73-83.

Sundar, L. S., M. K. Singh, E. V. Ramana, B. Singh, J. Gracio and A. C. M. Sousa (2014b). Enhanced thermal conductivity and viscosity of nanodiamond-Nickel nanocomposite nanofluids. *Scientific reports* 4, 4039.

Sundar, L. S., M. K. Singh, M. C. Ferro and A. C. M. Sousa (2017b). Experimental investigation of the thermal transport properties of graphene oxide/CO_3O_4 hybrid nanofluids. *Inter. Commun. in Heat and Mass Transf.* 84, 1-10.

Suresh, S., K. P. Venkitaraj, P. Selvakumar and M. Chandrasekar (2011). Synthesis of Al_2O_3-Cu/water hybrid nanofluids using two step method and its thermo physical properties. *Colloids and Surfaces A: Physicochem. Eng. Aspects* 388, 41-48.

Suresh, S., K. P. Venkitaraj, P. Selvakumar and M. Chandrasekar (2012). Effect of Al_2O_3–Cu/water hybrid nanofluid in heat transfer. *Exp. Thermal and Fluid Sci*. 38, 54-60.

Toghrai, D., V. A. Chaharsoghi and M. Afrand (2016). Measurement of thermal conductivity of ZnO–TiO_2/EG hybrid nanofluid. *J Therm Anal Calorim* 125, 527-535.

Vafaei, M., M. Afrand, N. Sina, R. Kalbasi, F. Sourani and H. Teimouri (2017). Evaluation of thermal conductivity of MgO-MWCNTs/EG hybrid nanofluids based on experimental data by selecting optimal artificial neural networks. *Physica E* 85, 90-96.

Wei, W., J. Cai, X. Hu, Q. Han, S. Liu and Y. Zhou (2016). Fractal analysis of the effect of particle aggregation distribution on thermal conductivity of nanofluids. *Physics Letters A* 380, 2953-2956.

Xiao, B., Y. Yang and L. Chen (2013). Developing a novel form of thermal conductivity of nanofluids with Brownian motion effect by means of fractal geometry. *Powder Technology* 239, 409-414.

Zareie, A. and M. Akbari (2017). Hybrid nanoparticles effects on rheological behaviour of water-EG coolant under different temperatures: An experimental study. *J. of Molecular Liquids* 230, 408-414.